Nonisothermal Crystallization Kinetics of Polypropylene/Polypropylene-*g*-Polystyrene/Polystyrene Blends

Jinge Li,[1,2] **Huayi Li,**[1] **Yucai Ke,**[1] **Qian Li,**[1] **Liaoyun Zhang,**[2] **Youliang Hu**[1]

[1]*Beijing National Laboratory for Molecular Sciences, Chinese Academy of Sciences Key Laboratory of Engineering Plastics, Joint Laboratory of Polymer Science and Materials, Institute of Chemistry, Chinese Academy of Sciences, Beijing 100190, China*
[2]*Graduate School, Chinese Academy of Sciences, Beijing 100049, China*

ABSTRACT: The nonisothermal crystallization kinetics of polypropylene (PP), PP/polystyrene (PS), and PP/PP-*g*-PS/PS blends were investigated with differential scanning calorimetry at different cooling rates. The Jeziorny modified Avrami equation, Ozawa method, and Mo method were used to describe the crystallization kinetics for all of the samples. The kinetics parameters, including the half-time of crystallization, the peak crystallization temperature, the Avrami exponent, the kinetic crystallization rate constant, the crystallization activation energy, and the $F(T)$ and a parameters were determined. All of the results clearly indicate that the PP-*g*-PS copolymer accelerated the crystallization rate of the PP component in the PP/PP-*g*-PS/PS blends. © 2010 Wiley Periodicals, Inc. J Appl Polym Sci 119: 1721–1731, 2011

Key words: blends; crystallization; graft copolymers; poly(propylene)(PP); polystyrene

INTRODUCTION

Since commercial production began in 1957, polypropylene (PP) has become one of the most widely used polymer resins because of its low price, low density, and high performance with regard to its mechanical and thermal properties, chemical resistance, and so on. However, its inherently low impact strength and low polarity limits PP applications and performance in wider fields. Polymer blending technology, which has always been an attractive alternative for the production of new polymeric materials with desirable properties, has been intensively applied in PP-based polymer blends in the development of new materials. For example, PP/PP-*g*-PS/PS polymer blends produced by Hivalloy technology have been reported with an excellent balance of stiffness and impact strength.[1–3] General speaking, PP and PS are typically incompatible binary blends because of their polarity and great differences of their polymer chains. Their blends usually result in serious phase separation, low interfacial adhesion, and poor mechanical properties. As a compatibilizer, the PP-*g*-PS copolymer actually improves the interfacial adhesion and produces a finer dispersion mixing of PP/PP-*g*-PS/PS polymer blends and, thus, enhances the mechanical properties.[4–11] Researchers have reported the development of morphologies and the rheological and isothermal crystallization behaviors of PP/PP-*g*-PS/PS polymer blends in detail. However, reports on the nonisothermal crystallization behavior of the PP/PP-*g*-PS/PS blend system have been comparatively fewer. This might be because of the simple theoretical analysis of the isothermal crystallization process and the possible problems associated with the cooling rates (Φ's) and thermal gradients within specimens.[12] In practice, crystallization in continuously changing temperatures is much more similar to the industrial process; that is, the final material properties are correlated to the nonisothermal crystallization process. From a practical point of view, research on the nonisothermal crystallization process will provide useful information for the analysis and design of processing parameters from the investigation of the nonisothermal crystallization kinetics of the polymeric materials. Therefore, the study of nonisothermal crystallization for the PP/PP-*g*-PS/PS blend system is very important. In this study, the effect of the compatibilizer, PP-*g*-PS copolymer, on the nonisothermal crystallization processes, nucleation, and growth mechanisms and the crystallization activation energies (ΔE's) of PP/PS blends were systematically investigated.

EXPERIMENTAL

Isotactic PP [trade name S1003, number-average molecular weight (M_n)= 88,000, molecular weight

TABLE I
Composition of the PP/PS and PP/PP-*g*-PS/PS Blend Samples

Sample	PP-*g*-PS	PP	D0	D1	D3	D5	D9
$W_{PP\text{-}g\text{-}PS}/W_{PP}{}^a$	1	0		0.01	0.03	0.05	0.09
$W_{PP}/W_{PS}{}^b$		1	75/25	75/25	75/25	75/25	75/25

[a] Weight fraction of PP-*g*-PS copolymer in PP components.
[b] All the blend samples with the fixed weight ratio 75/25 of PP and PS components and the increasing content of PP-*g*-PS.

distribution = 3.7] and atactic PS (trade name 666D, M_n= 87,000, molecular weight distribution = 3.6) were purchased from Yanshan Petro-Chemical Co. (Beijing, China) and were used as received. The PP-*g*-PS copolymer was synthesized according to a previous report.[13] M_n and the polydispersity index (weight-average molecular weight/M_n) of the backbone of PP-*g*-PS, determined by high temperature gel permeation chromatography, were 3.6×10^4 g/mol and 4.5, respectively. Calculated according to
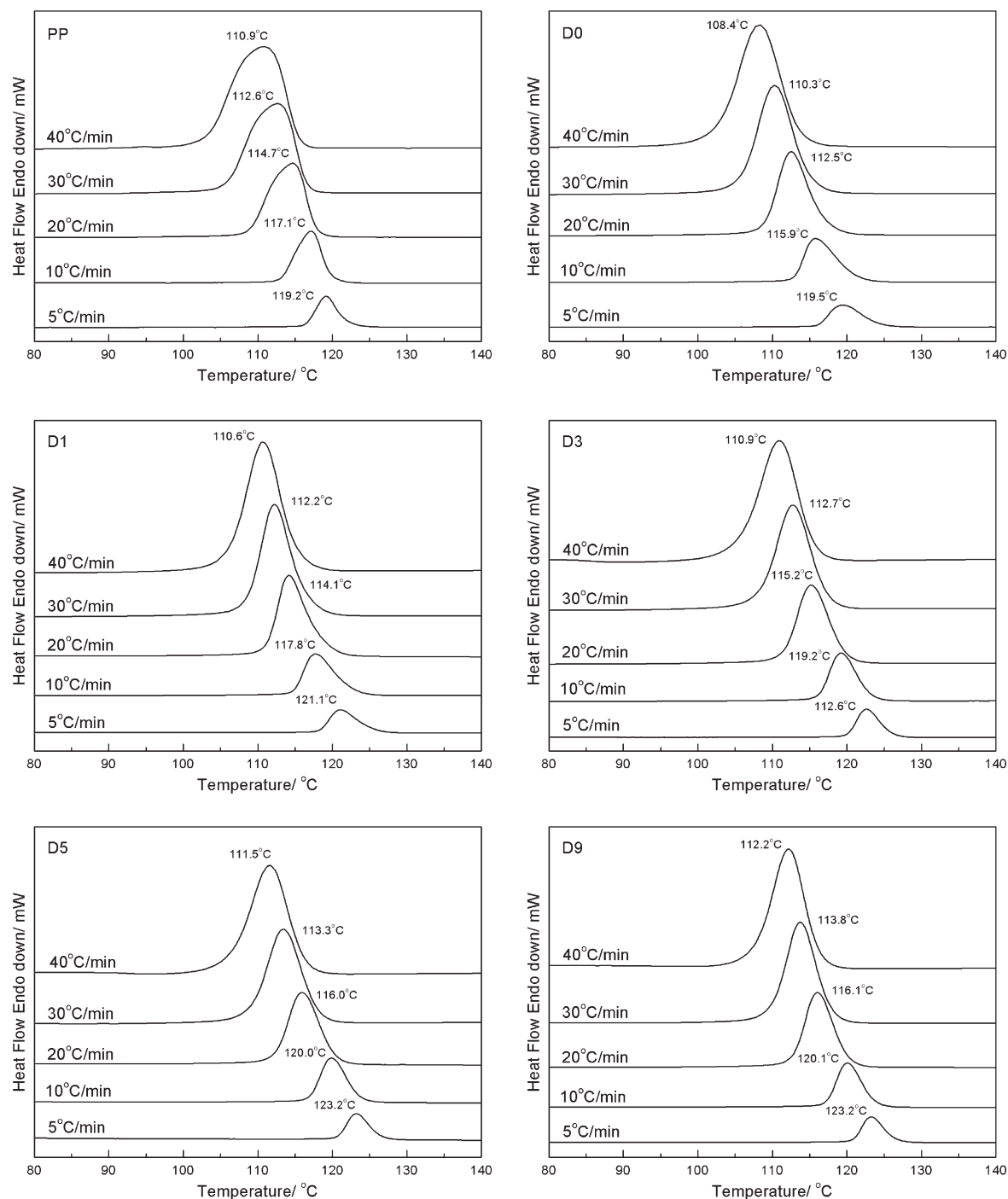

Figure 1 Crystallization exotherms of the PP and PP/PS and PP/PP-*g*-PS/PS blends at different Φ values.

TABLE II
T_p, T_o, and ΔH_c of the PP and PP/PS and PP/PP-*g*-PS/PS Blend Samples

Sample	Φ(°C/min)	T_o(°C)	T_p(°C)	ΔH_c(J/g)
PP	40	115.54	110.88	87.58
	30	116.59	112.63	88.54
	20	117.82	114.70	90.35
	10	119.77	117.10	92.02
	5	122.02	119.16	92.37
D0	40	113.53	108.41	73.66
	30	115.07	110.28	75.22
	20	117.11	112.49	76.38
	10	121.34	115.88	77.73
	5	124.37	119.51	78.66
D1	40	115.24	110.56	70.25
	30	116.56	112.20	72.37
	20	118.74	114.12	72.62
	10	122.73	117.79	75.37
	5	125.64	121.07	75.74
D3	40	115.58	110.93	65.98
	30	117.36	112.68	69.62
	20	119.79	115.19	71.13
	10	123.18	119.18	72.32
	5	126.11	122.62	72.77
D5	40	116.28	111.55	61.52
	30	118.07	113.34	68.54
	20	120.33	115.97	70.74
	10	123.66	119.88	72.93
	5	126.53	123.23	74.41
D9	40	116.23	112.17	62.55
	30	117.90	113.79	68.96
	20	120.16	116.07	71.53
	10	123.76	120.06	74.15
	5	126.55	123.24	74.63

^{1}H-NMR spectra, the *graft density*(defined as the average number of grafted side chains per 1000 carbons in the PP backbones) of the PP-*g*-PS copolymer was 3.15, the *average side length*(defined as the average degree of polymerization of the PS sequences) of the PP-*g*-PS copolymer was 60.2, and the weight ratio of styrene to propylene units was 1.21. PP, PS, and PP-*g*-PS were dry-blended by the addition of the antioxidant 1010 (Yingkou Viewchem Co., Ying-Kou, China) with a 0.5% weight ratio of the blends and were then mixed in a commercial single-screw extruder (Haake R90, USA). For the PP/PP-*g*-PS/PS blends, the weight ratio of PP to PS was fixed at 75/25, and the concentrations of the PP-*g*-PS copolymer were 1, 3, 5, and 9 wt % of the PP components. The compositions of the polymer blend samples are listed in Table I.

Nonisothermal crystallization kinetics of the sample were determined with a PerkinElmer DSC-7e (USA) instrument with nitrogen as a purge gas. Pure indium was used as a reference material to calibrate both the temperature scale and the melting enthalpy before the samples were tested. The samples ($\sim$ 5 mg) were preheated to 200°C for 5 min to eliminate any possible thermal history and were then cooled to 60°C at different Φ's of 40, 30, 20, 10, and 5°C/min, respectively. The heat flow during crystallization (dH_c/dT) was recorded as a function of temperature.

For optical microscopy observation, an Olympus (Japan) BX-51 optical microscope equipped with a hot stage (Linkam, THMS600, UK) was used. All of the optical micrographs were taken with a crossed polarizer.

RESULTS AND DISCUSSION

Nonisothermal crystallization behavior

The crystallization exotherms of plain PP and the PP/PS and PP/PP-*g*-PS/PS blends at various Φ's are shown in Figure 1. Each curve showed a distinct exothermic crystallization peak. The peak crystallization temperature (T_p), onset temperature of crystallization (T_o), and enthalpy of crystallization (ΔH_c) of the PP and PP/PS and PP/PP-*g*-PS/PS blend samples determined from these curves are listed in Table II. For all of the investigated samples, the PP chains had enough time to fold into lamellar crystals, whereas Φ became slower; therefore, decreasing values of T_o, T_p, and ΔH_c were observed with increasing Φ. As reported in Table II, the values of T_o and T_p increased from samples D1 to D9, whereas the values of these parameters for sample D1 were not different from the corresponding parameters for the unblended PP, and for sample D0, both T_o and T_p decreased from their values for unblended PP. This decrease indicated a slowing of the nucleation rates and overall crystallization of PP on addition of PS. This trend reversed on addition of the third component, PP-*g*-PS. Clearly, the graft copolymer accelerated the crystallization rate of the PP component in the ternary blend system; therefore, T_o and T_p shifted to higher temperatures. More details can be obtained from the optical micrographs shown in Figure 2. The optical micrographs were taken at the crossed polarizer of the thin films of the PP/PS binary and PP/PP-*g*-PS/PS ternary blend isothermally crystallized at 130°C. For comparison, here we only displayed the micrographs of D0 and D5 as examples at early and final crystallization stages. As shown in Figure 2, the dispersed particles were the PS component. Heterogeneous nucleation occurred on the surfaces of the PS particles in both of the samples with or without PP-*g*-PS as a compatibilizer. The PP-*g*-PS copolymer improved the distribution of the PS dispersed phase in D5; that is, PS dispersed particles became smaller and more regular, and then, more heterogeneous nucleation sites were introduced into the blend sample; therefore, T_o and T_p shifted to higher
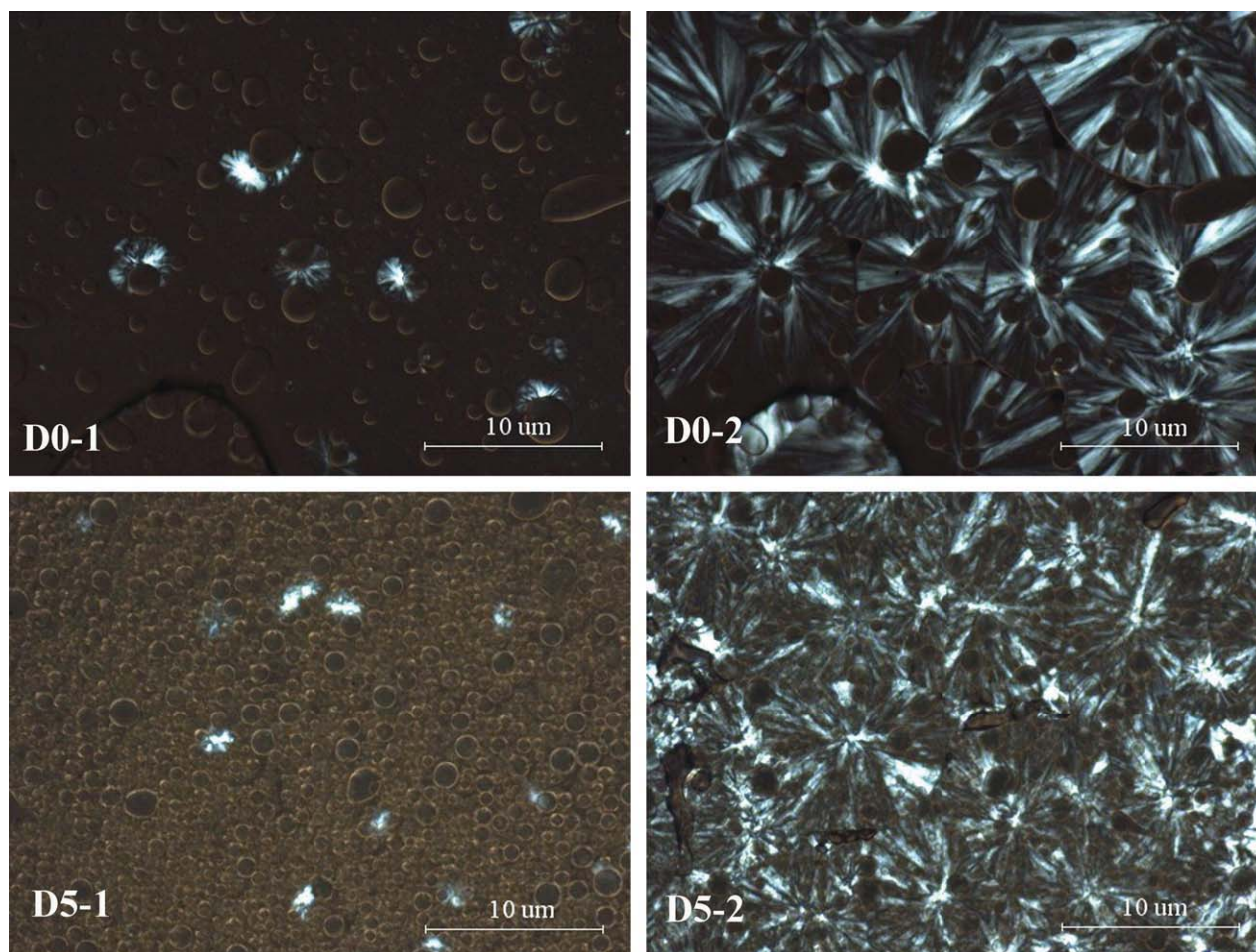
Figure 2 Optical micrographs of the PP/PS binary blend (D0) and PP/PP-*g*-PS/PS ternary blend (D5) isothermally crystallized at 130°C. [Color figure can be viewed in the online issue, which is available at wileyonlinelibrary.com.]

temperatures. The two parameters T_o and T_p may be viewed as distinguishing the effect of the two steps of crystallization process, namely, nucleation and growth, as described in the literature.[14] T_o was neatly affected by the initial step (nucleation), whereas T_p may have had combined influence from both steps (nucleation and growth). In the light of this, the observed effect of PS and PP-*g*-PS on the nucleation and overall crystallization (i.e., combined process of nucleation followed by growth) could be inferred from the data obtained. The PP-*g*-PS copolymer accelerated the crystallization rate of the PP component by improving the distribution of PS particles. The PS component provided heterogeneous nucleation sites in all of the blend samples. However, because of a dilution effect that influenced the diffusion of the macromolecules, the PS particles also hindered the growth of PP crystals to some extent. Therefore, the effect of the PS component in the blend samples included two inversed factors in the crystallization process, namely, nucleation and growth.

According to the values of ΔH_c at a given Φ for all of the investigated samples, both PP-*g*-PS and the PS component decreased the relative crystallinity of PP. D'Orazio et al.[9] reported similar results in their previous article. The presence in the melt of segregated PS domains interfered with the PP crystallization process and then decreased the PP crystallinity. On the other hand, PP-*g*-PS also interfered with the PP crystallization process[15] and enhanced the interference of PS domains on the PP crystallization process because of the improved compatibility of the PS and PP components.

Nonisothermal crystallization kinetics

The relative degree of crystallinity (X_t) as a function of crystallization temperature (T) is defined as

$$X_t = \frac{\int_{T_o}^{T} \frac{dH_c}{dT} dT}{\int_{T_o}^{T_\infty} \frac{dH_c}{dT} dT} \tag{1}$$

where T_∞ is the end temperature of crystallization. Figure 3 shows the development of X_t as a function
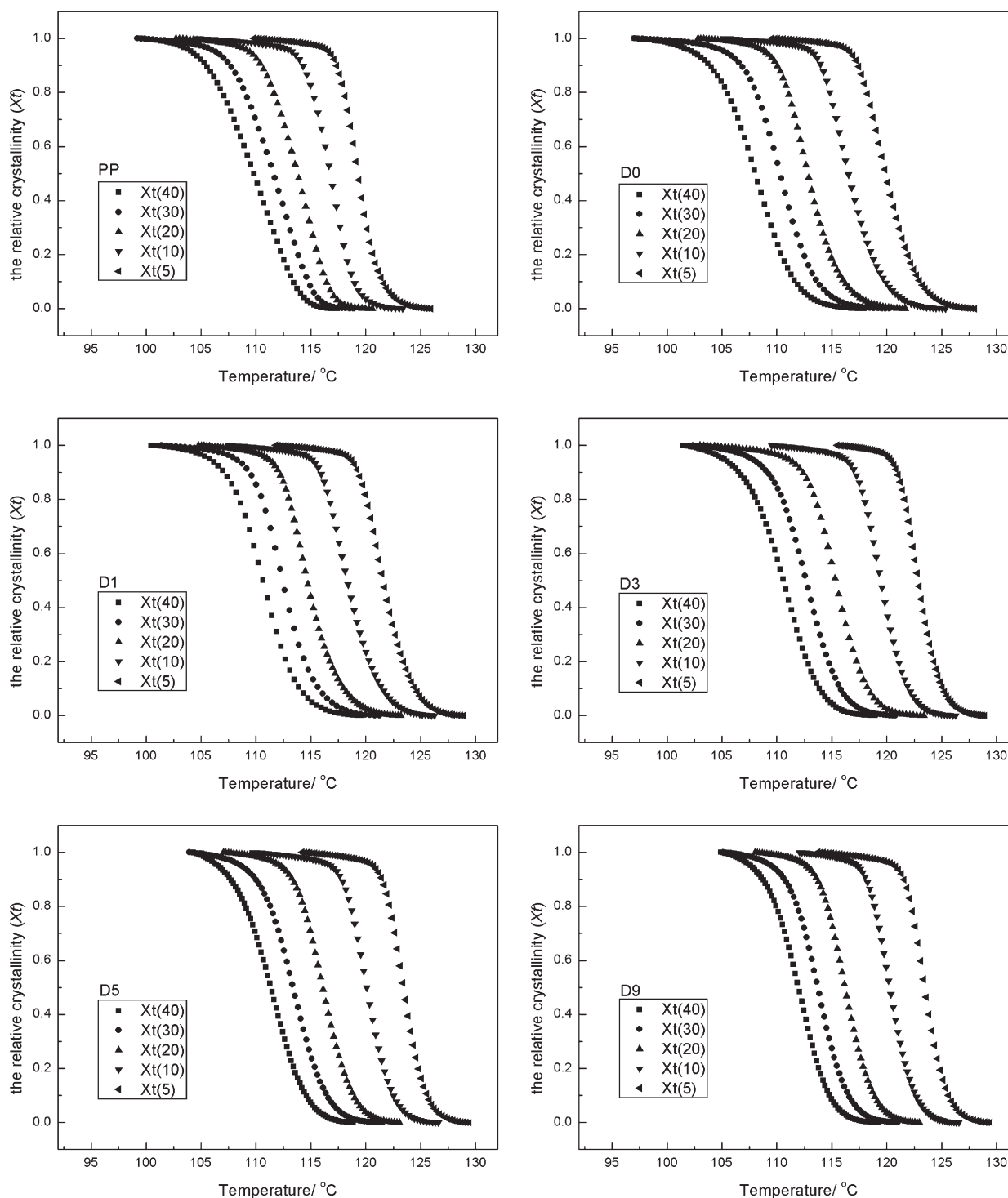
Figure 3 Relative crystallinity versus the temperature during the nonisothermal crystallization process of the PP and PP/PS and PP/PP-*g*-PS/PS blends.

of temperature for the plain PP and the PP/PS and PP/PP-*g*-PS/PS blend samples at various Φ's. Clearly, all of these curves had the same sigmoidal shape; this implied that only the lag effect of Φ on crystallization was observed for these curves. For the nonisothermal crystallization process recorded by differential scanning calorimetry measurement, the temperature axis shown in Figure 3 could

be transformed into timescale with the following equation:

$$t = \frac{T_o - T}{\Phi} \quad (2)$$

where t is the corresponding crystallization time at T. According to eqs. (1) and (2), the dependence of X_t on
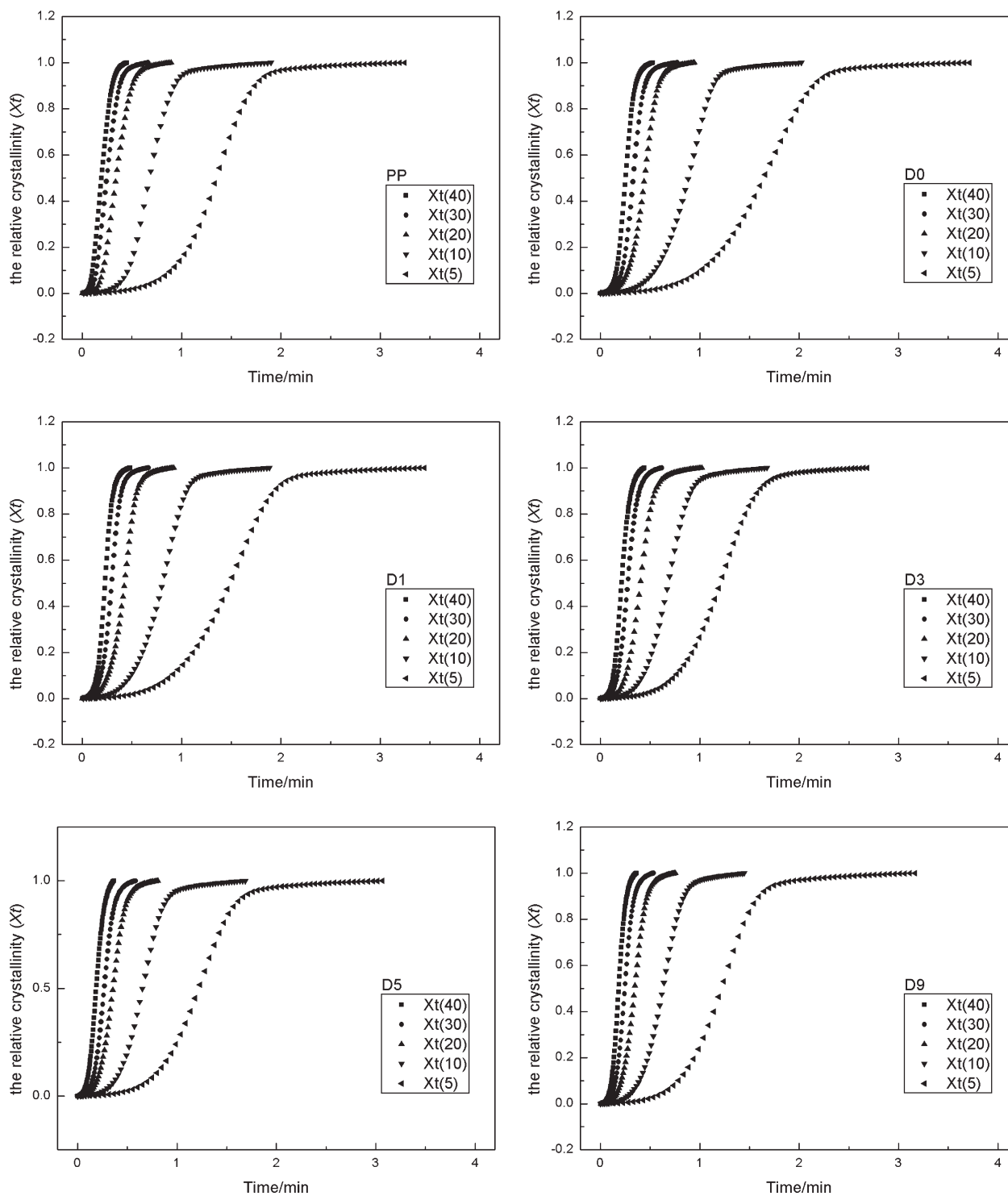
Figure 4 Relative crystallinity versus the time during the nonisothermal crystallization process of the PP and PP/PS and PP/PP-*g*-PS/PS blends.

t at a given Φ is shown in Figure 4. The time required for the complete crystallization of PP tended to be shorter with increasing Φ from 5 to 40°C/min. The half-time of crystallization ($t_{1/2}$) can be obtained from Figure 4 at $X_t = 0.5$, and the results are listed in Table III. As shown by these values, the $t_{1/2}$ values increased with decreasing Φ for all of the investigated

samples. Also, for the PP/PS binary and PP/PP-*g*-PS/PS ternary blend samples, the $t_{1/2}$ values decreased significantly at a given Φ with increasing PP-*g*-PS content; this suggested that the graft copolymer accelerated the overall crystallization process.

The nonisothermal crystallization kinetics usually can be analyzed with the Avrami equation as follows:[15,16]

TABLE III
Nonisothermal Crystallization Kinetic Parameters for the PP and PP/PS and PP/PP-g-PS/PS Blend Samples

Sample	$\Phi(°C/min)$	$t_{1/2}(min)$	k	n	k_c
PP	40	0.19	50.94	2.6	1.10
	30	0.25	35.76	2.8	1.13
	20	0.34	22.13	3.2	1.17
	10	0.68	3.84	4.4	1.14
	5	1.35	0.15	5.2	0.68
D0	40	0.25	137.84	3.8	1.13
	30	0.33	103.53	4.5	1.17
	20	0.45	28.26	4.6	1.18
	10	0.88	1.19	4.4	1.02
	5	1.64	0.08	4.4	0.60
D1	40	0.23	389.68	4.3	1.16
	30	0.30	192.98	4.7	1.19
	20	0.43	35.04	4.6	1.19
	10	0.81	1.75	4.3	1.06
	5	1.49	0.12	4.3	0.66
D3	40	0.22	183.00	3.6	1.14
	30	0.28	111.80	3.9	1.17
	20	0.40	32.93	4.2	1.19
	10	0.68	3.56	4.3	1.14
	5	1.21	0.30	4.4	0.79
D5	40	0.19	181.04	3.3	1.14
	30	0.27	120.53	3.9	1.17
	20	0.35	39.50	3.9	1.20
	10	0.65	4.25	4.3	1.16
	5	1.22	0.28	4.6	0.78
D9	40	0.18	156.38	3.8	1.17
	30	0.25	95.56	4.0	1.19
	20	0.35	33.29	4.1	1.22
	10	0.63	3.42	4.3	1.18
	5	1.22	0.16	4.6	0.77

$$1 - X_t = \exp(-kt^n) \qquad (3)$$

where k is a composite rate constant involving both nucleation and growth rate parameters and n is the Avrami exponent and depends on the type of nucleation and growth process. Equation (3) can be written in double-logarithmic form as follows:

$$\ln[-\ln(1 - X_t)] = \ln k + n \ln t \qquad (4)$$

According to eq. (4), the plot of $\ln[-\ln(1 - X_t)]$ against $\ln t$ for all of the investigated samples at each Φ will yield a straight line with slope n and intercept $\ln k$. However, the linearity relationship only existed at low X_t, as shown in Figure 5, and all the data diverged from the straight line at the complete stage of crystallization. Generally, this deviation was due to secondary crystallization. The linear portions were almost parallel to each other and shifted to shorter time with increasing Φ. These results imply that the nucleation mechanism and crystal growth geometries of primary crystallization were similar for all of the samples. The calculated values of n and k for all of the investigated samples are listed in Table III. Generally, n in the crystallization of polymers includes the crystallization

mechanism, sporadic and predetermined, and the space dimension of the spheres.[12,17] Thus, the n values ranged from 2.6 to 5.2; these values suggested heterogeneous nucleation for all of the samples, in agreement with Figure 2. For the PP/PP-g-PS/PS ternary blend samples, the values of k increased gradually with increasing content of PP-g-PS at each Φ; this indicated an acceleration effect of the graft copolymer in the crystallization processes of the blend samples.

According to the nonisothermal character of the process investigated, the value of k should have been modified by Φ. According to the Jeziorny method,[18] the final form of the rate constant is given as follows

$$\ln k_c = \ln k / \Phi \qquad (5)$$

where k_c is the kinetic crystallization rate constant. As shown in Table III, the values of k_c ranged from 1.1 to 1.2 for all of the investigated samples at Φ's from 40 to 10°C/min and ranged from 0.6 to 0.8 at a Φ of 5°C/min. These results confirm similar nucleation mechanisms and crystal growth geometries for all of the samples.

With the Φ dependence on the nonisothermal crystallization process taken into consideration, Ozawa[19] modified the Avrami equation as follows:

$$1 - X_t = \exp[-\frac{K(T)}{\Phi^m}] \qquad (6)$$

where $K(T)$ is the function of Φ related to the overall crystallization rate and m is the Ozawa exponent, which depends on the dimensions of crystal growth. The double-logarithmic form of eq. (6) is given as follows:

$$\ln[-\ln(1 - X_t)] = \ln K(T) - m \ln \Phi. \qquad (7)$$

According to eq. (7), the plot of $\ln[-\ln(1 - X_t)]$ versus $\ln \Phi$ for the samples will yield a straight line at a given T. However, many reports have confirmed that the plot usually does not exhibit a linear relationship with the Ozawa method, especially for semicrystalline polymer.[12,20–22] This is probably due to the ignorance of secondary crystallization and the dependence of the fold length on the temperature.[12] Figure 6 shows the plots of $\ln[-\ln(1 - X_t)]$ versus $\ln \Phi$ for all of the samples. Clearly, the curves were not linear lines at each T. Therefore, it was not suitable to analyze the crystallization process of plain PP or the PP components in the blend samples with the Ozawa method. Another improved method was reported by Mo et al.[17] Because the crystallization is related to Φ and t (or T), the relationship between Φ and t at a given crystallinity can be built up by a combination of the Avrami equation with the Ozawa equation as follows:
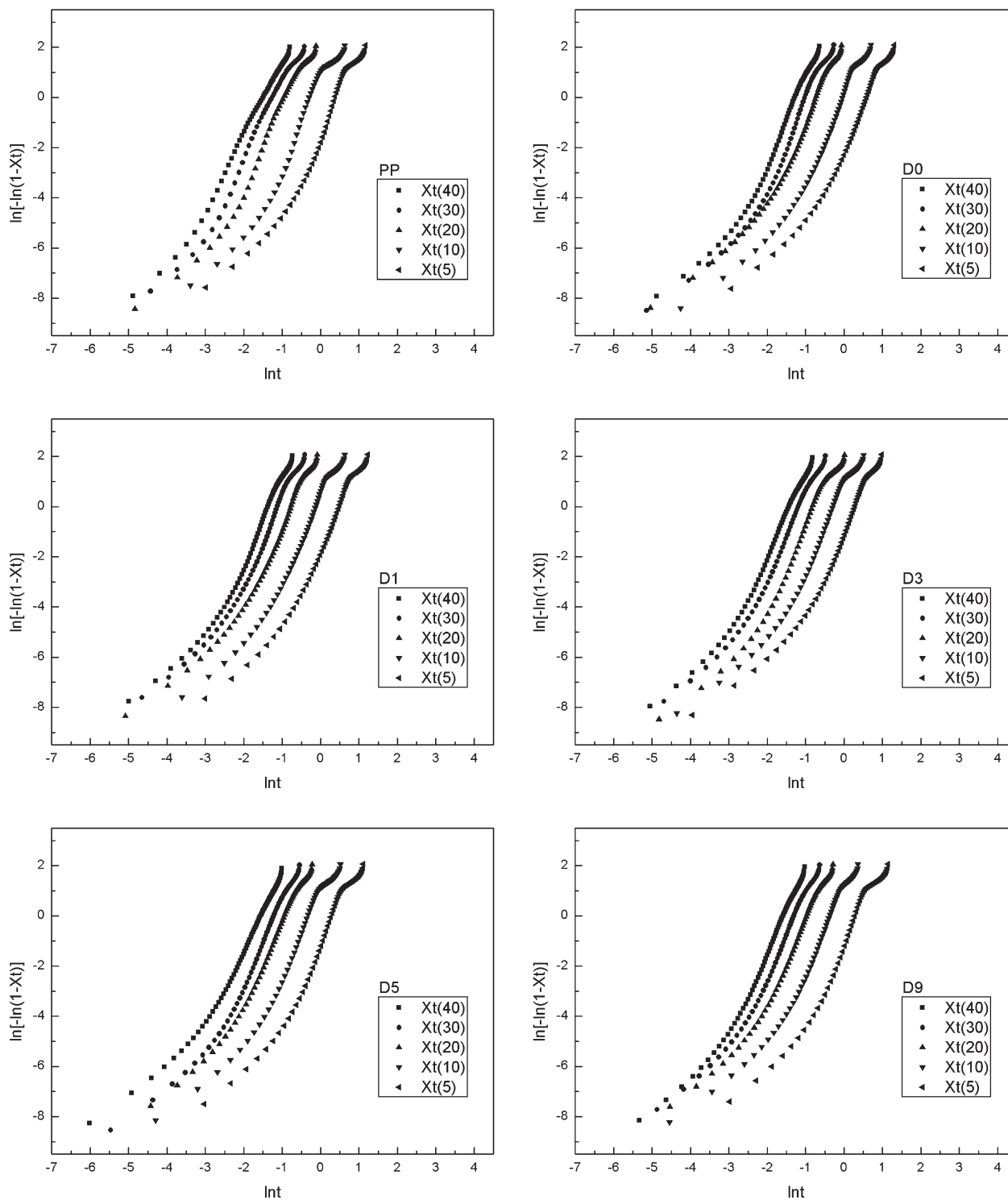
Figure 5 Plots of ln[−ln(1 − Xt)] versus ln t for the nonisothermal crystallization process of PP and PP/PS and PP/PP-g-PS/PS blends.

$$\ln[-\ln(1 - X_t)] = \ln k + n \ln t = \ln K(T) - m \ln \Phi \quad (8)$$

then

$$\ln \Phi = \ln F(T) - a \ln t \quad (9)$$

where the kinetic parameter $F(T) = [K(T)/k]^{1/m}$ refers to the value of Φ, which must be chosen at unit t when the measured system amounts to a certain X_t, and a is the ratio of n to m. As shown in Figure 7, all plots of ln Φ against ln t for the samples gave a series of straight lines at a given
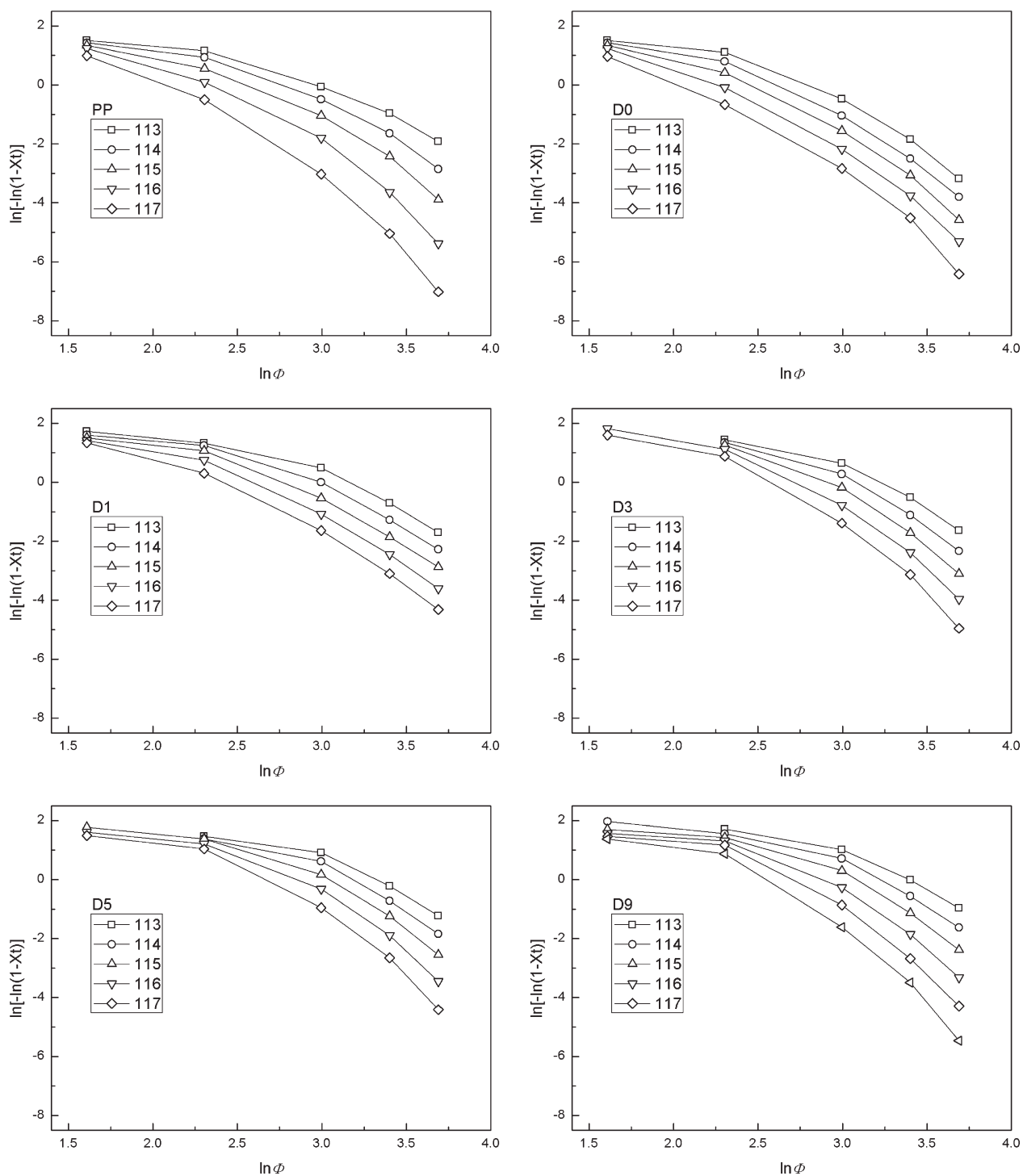
Figure 6 Ozawa plots of ln[−ln(1 − Xt)] versus ln Φ for the nonisothermal crystallization process of the PP and PP/PS and PP/PP-*g*-PS/PS blends.

X_t. The kinetic parameters $F(T)$ and a, estimated by the intercepts and the slopes of these lines, respectively, are listed in Table IV. As shown by these data, the values of $F(T)$ systematically increased with the relative X_t. The values of a were in the range 0.8–1.0 and were almost equal to a constant value. For the PP/PP-*g*-PS/PS blend samples, the values of $F(T)$ decreased with increas-

ing PP-*g*-PS content; therefore, the crystallization rate increased with increasing PP-*g*-PS content.

ΔE

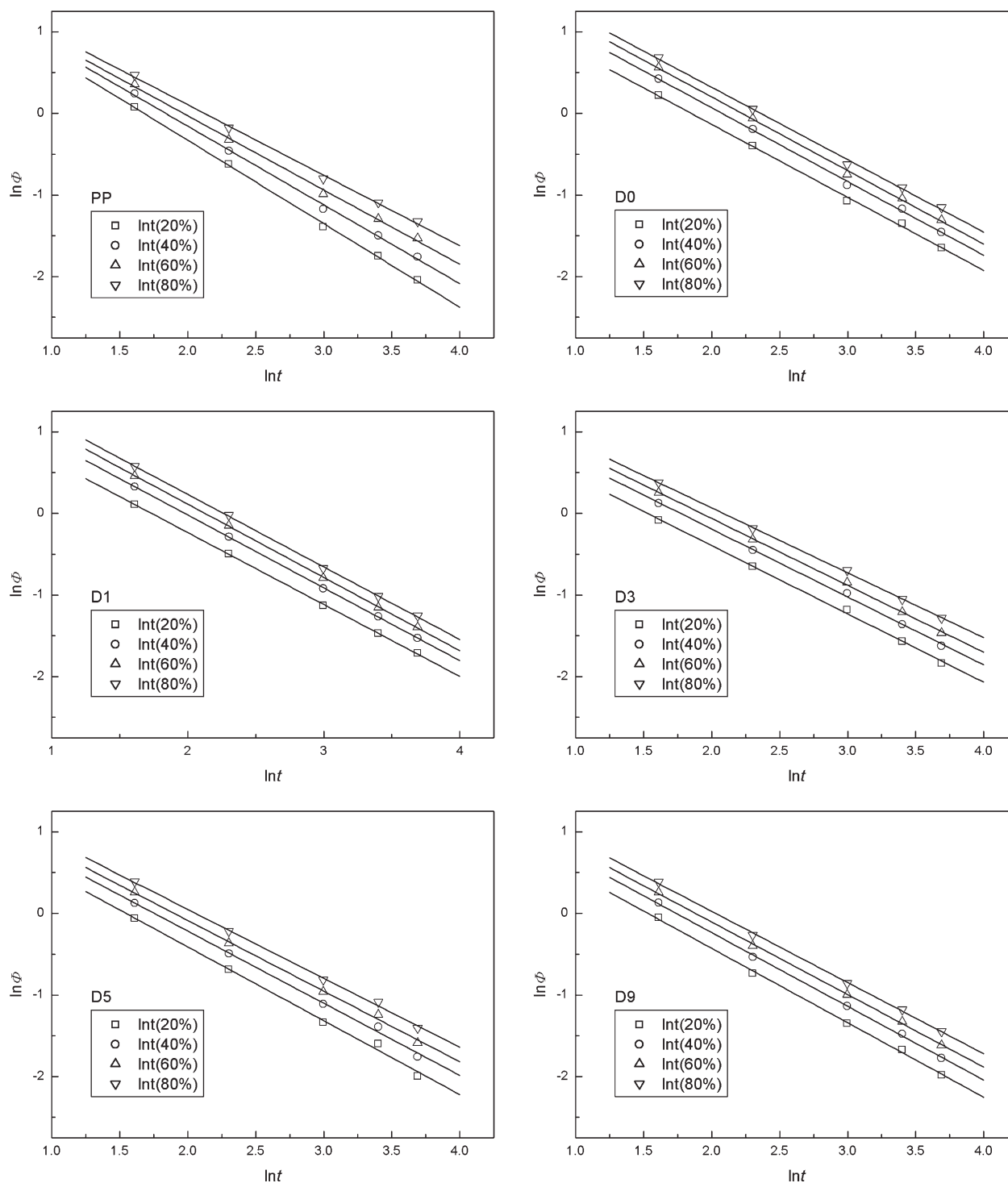With the variation of T_p with Φ taken into consideration, ΔE, can be determined by the Kissinger equation:[23]

Figure 7 Plots of ln[−ln(1 − Xt)] versus ln Φ on the basis of the Mo equation for the nonisothermal crystallization process of the PP and PP/PS and PP/PP-g-PS/PS blends.

$$\frac{d[\ln(\Phi/T_p^2)]}{d(1/T_p)} = -\frac{\Delta E}{R} \qquad (10)$$

where R is the universal gas constant. Accordingly, the plots of $\ln(\Phi/T_p^2)$ versus $1/T_p$ for all of the samples are shown in Figure 8. The ΔE values were calculated by the slopes of the fitting lines and are

listed in Table IV. For the PP/PP-g-PS/PS blend samples, the values of ΔE decreased with increasing PP-g-PS content. Such a result also clearly indicated that the PP-g-PS copolymer accelerated the crystallization rate of PP in the ternary blend system. On the other hand, when the blend samples was compared with the unblended PP, especially for PP and D0, the values of ΔE from the unblended PP were bigger

TABLE IV
Different Crystallization Kinetic Parameters and ΔE Values of the PP and PP/PS and PP/PP-g-PS/PS Blend Samples

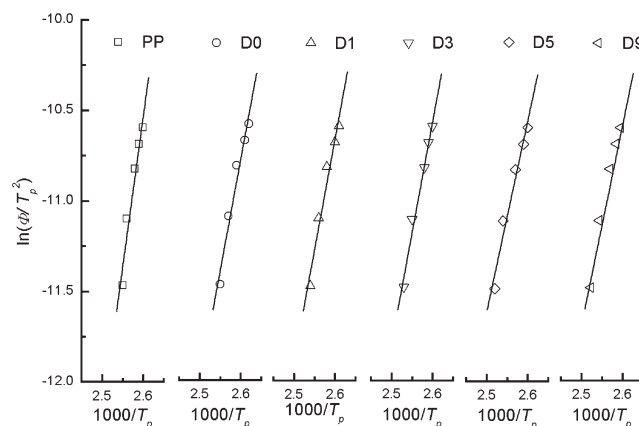| Sample	$X_t(\%)$	$F(T)$	a	$-\Delta E$(kJ/mol)
PP	20	5.56	1.0	129.28
	40	5.88	1.0	
	60	5.99	0.9	
	80	6.25	0.9	
D0	20	5.22	0.9	100.05
	40	6.52	0.9	
	60	7.42	0.9	
	80	9.12	0.9	
D1	20	4.6	0.9	104.84
	40	5.84	0.9	
	60	6.74	0.9	
	80	7.46	0.9	
D3	20	3.59	0.8	94.46
	40	4.37	0.8	
	60	4.84	0.8	
	80	5.24	0.8	
D5	20	4.05	0.9	94.62
	40	4.71	0.9	
	60	5.17	0.9	
	80	5.69	0.9	
D9	20	4.03	0.9	92.15
	40	5.81	0.9	
	60	5.32	0.9	
	80	5.87	0.9	

Figure 8 Plots of $\ln(\Phi/T_p^2)$ versus $1/T_p$ based on the Kissinger equation for the nonisothermal crystallization process of the PP and PP/PS and PP/PP-g-PS/PS blends.

content in the PP/PP-g-PS/PS blend samples. This also proved that the PP-g-PS copolymer accelerated the crystallization rate of the PP component in the PP/PP-g-PS/PS blends.

than those of the other samples; that is, the PS component in the whole crystallization process improved the crystallization rate in all of the blend samples.

CONCLUSIONS

In this study, the nonisothermal crystallization kinetics of PP and PP/PS and PP/PP-g-PS/PS blends were investigated with differential scanning calorimetry measurements. When we compared the $t_{1/2}$ values of the samples at a given Φ, we observed that the PP-g-PS copolymer accelerated the crystallization rate of PP in the blend systems. Furthermore, Avrami analysis pointed out that all of the investigated samples showed a similar nucleation mechanism and crystal growth geometries at the primary crystallization stage. The n values ranged from 2.6 to 5.2, and optical microscopy observation suggested heterogeneous nucleation for all of the samples at the primary crystallization stage. The Ozawa method was proven to be invalid for describing the nonisothermal crystallization of PP and the blend samples. However, the Mo method was satisfactory for correlating Φ to T and t. ΔE was estimated by the Kissinger equation. As expect, the values of the activation energy decreased with increasing PP-g-PS

References

1. Galli, P.; Collina, G.; Sgarzi, P.; Baruzzi, C.; Marchetti, E. J Appl Polym Sci 1997, 66, 1831.
2. Galli, P. J Macromol Sci Phys 1996, 35, 427.
3. Cecchin, G.; Morini, G.; Pelliconi, A. Macromol Symp 2001, 173, 195.
4. Caporaso, L.; Iudici, N.; Oliva, L. Macromolecules 2005, 38, 4894.
5. Diaz, M. F.; Barbosa, S. E.; Capiati, N. J. J Polym Sci Part B: Polym Phys 2004, 42, 452.
6. Picchioni, F.; Goossens, J. G. P.; van Duin, M. J Appl Polym Sci 2005, 97, 575.
7. Park, E. S.; Jin, H. J.; Lee, I. M.; Kim, M. N.; Lee, H. S.; Yoon, J. S. J Appl Polym Sci 2002, 83, 1103.
8. D'Orazio, L.; Guarino, R.; Mancarella, C.; Martuscelli, E.; Cecchin, G. J Appl Polym Sci 1997, 65, 1539.
9. D'Orazio, L.; Guarino, R.; Mancarella, C.; Martuscelli, E.; Cecchin, G. J Appl Polym Sci 1999, 72, 1429.
10. Adewole, A. A.; DeNicola, A.; Gogos, C. G.; Mascia, L. Plast Rubber Compos 2000, 29, 70.
11. Adewole, A. A.; Denicola, A.; Gogos, C. G.; Mascia, L. Adv Polym Technol 2000, 19, 180.
12. Nandi, S.; Ghosh, A. K. J Polym Res 2007, 14, 387.
13. Li, J. G.; Li, H. Y.; Wu, C. H.; Ke, Y. C.; Wang, D. J.; Li, Q.; Zhang, L. Y.; Hu, Y. L. Eur Polym J 2009, 45, 2619.
14. Jafari, S. H.; Gupta, A. K. J Appl Polym Sci 1999, 71, 1153.
15. Avrami, M. J Chem Phys 1939, 7, 1103.
16. Avrami, M. J Chem Phys 1940, 8, 212.
17. Liu, T.; Mo, Z.; Zhang, H. J Appl Polym Sci 1998, 67, 815.
18. Fedors, R. F.; Landel, R. F. Polymer 1978, 19, 1189.
19. Ozawa, T. Polymer 1971, 12, 150.
20. Eder, M.; Wlochowicz, A. Polymer 1983, 24, 1593.
21. Gopakumar, T. G.; Lee, J. A.; Kontopoulou, M.; Parent, J. S. Polymer 2002, 43, 5483.
22. Durmus, A.; Yalcinyuva, T. J Polym Res 2009, 16, 489.
23. Kissinger, H. E. J Res Natl Bur Stand 1956, 57, 217.